CONF-8903109--2

LBL-26652

Center for Advanced Materials

CAM

To be presented at the 5th International Aluminum-Lithium Conference, Williamsburg, VA, March 28–31, 1989

Cryogenic Mechanical Properties of Low Density Superplastically Formable Al-Li Alloys

S.L. Verzasconi and J.W. Morris, Jr.

March 1989

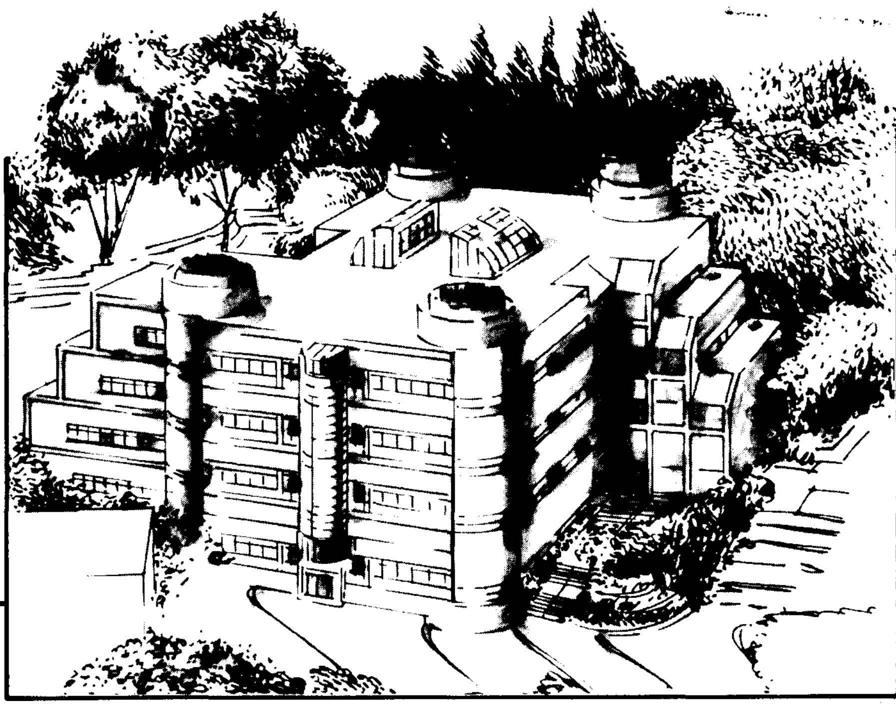

Materials and Chemical Sciences Division

Lawrence Berkeley Laboratory • University of California

ONE CYCLOTRON ROAD, BERKELEY, CA 94720 • (415) 486-4755

Prepared for the U.S. Department of Energy under Contract DE-AC03-76SF00098

LBL--26652

DE89 010587

CRYOGENIC MECHANICAL PROPERTIES OF LOW DENSITY SUPERPLASTICALLY FORMABLE AL-LI ALLOYS

S. L. Verzasconi and J. W. Morris, Jr.

Department of Materials Science and Mineral Engineering
University of California

and

Center for Advanced Materials
Materials and Chemical Sciences Division
Lawrence Berkeley Laboratory
1 Cyclotron Road
Berkeley, CA 94720

March 1989

This work was supported by Director, Office of Energy Research, Office of Basic Energy Sciences, Materials Science Divison of the U. S. Department of Energy under Contract No. *DE-AC03-76SF00098*

CRYOGENIC MECHANICAL PROPERTIES OF LOW DENSITY SUPERPLASTICALLY FORMABLE AL-LI ALLOYS.

S. L. Verzasconi and J.W. Morris, Jr.

Center for Advanced Materials, Lawrence Berkeley Laboratory and
Department of Materials Science and Mineral Engineering,
University of California, Berkeley.

ABSTRACT

The aerospace industry is considering the use of low density, superplastically formable (SPF) materials, such as Al-Li alloys in cryogenic tankage. SPF modifications of alloys 8090, 2090, and 2090+In were tested for strength and Kahn tear toughness. The results were compared to those of similar tests of 2219-T87, an alloy currently used in cryogenic tankage, and 2090-T81, a recently studied Al-Li alloy with exceptional cryogenic properties (1-9). With decreasing temperature, all materials showed an increase in strength, while most materials showed an increase in elongation and decrease in Kahn toughness. The indium addition to 2090 increased alloy strength, but did not improve the strength-toughness combination. The fracture mode was predominantly intergranular along small, recrystallized grains, with some transgranular fracture, some ductile rupture, and some delamination on large, unrecrystallized grains.

INTRODUCTION

Superplastically formable aluminum-lithium alloys are currently being considered for use in cryogenic fuel tanks. Superplastically formed structures can be more efficient than conventional milled structures because they reduce material waste and because complicated parts can be formed to support more load for given weight. Al-Li alloys are candidates for space vehicles because they have lower density and higher elastic modulus than conventional aerospace alloys; furthermore, some Al-Li alloys exhibit exceptional properties at cryogenic temperatures (1-9).

Although the design criteria and property limits have not yet been agreed upon, interest was expressed at NASA Langley and Northrop Aerospace Corporation in the strength and toughness of several superplastically formable Al-Li alloys, some of which included an indium addition to alloy 2090. Indium has previously been shown to improve the hardness of aluminum alloys (10); thus it was proposed to improve alloy strength. A strength boost is desired because the superplastic condition cannot include the stretch that improves alloy strength and toughness from the T6 to the T8 condition in aluminum-lithium alloys. Indium, like the mechanical stretch, is believed to encourage more uniform nucleation of the strengthening phases in these alloys (10-12).

Several candidate alloys were tested for strength and toughness at 300 and 77 K, including 2090, 8090, 2090+In, and 2219, mostly in sheet form. A toughness indicator test, the Kahn tear, was used both because the cryogenic test facility available for 4 K testing was not large enough to contain a center-cracked toughness specimen and because of the large existing data base on aluminum alloys tested with this method (13). The Kahn tear test provides two toughness indicators, the unit propagation energy (UPE) and the tear strength to yield strength ratio (tear-yield ratio). The UPE is the energy to propagate the crack per unit area, determined by dividing the area under the load-displacement curve after peak load (after the point of crack initiation) by the specimen ligament. Tear-yield ratio is the ratio of the tear strength, or maximum strength, which occurs just before crack initiation, to the 0.2 % offset yield strength. The following report is a summary of the mechanical test results and microstructural analysis conducted at Lawrence Berkeley Laboratory (LBL) as part of a joint research effort with NASA and Northrop.

EXPERIMENTAL PROCEDURE

Materials.

The alloys tested included 2090-T6, 8090-T6, three thermal conditions from two lots of 2090+In, 2090-T81, and 2219-T87. Table 1 contains the compositions in weight percent of the superplastic sheet materials, cast at Reynolds Aluminum, along with reference material 2090-T81, cast and processed at Alcoa and chemically analyzed at Anamet. The second lot of 2090+In was produced to lower the iron and silicon content, since these elements are detrimental to both the mechanical properties and the superplastic formability of aluminum-lithium alloys (14, 15). The reference materials used included 2090-T81, which came from a 1.27 cm (0.5 inch) plate, and 2219-T87 in 0.318 cm (0.125 inch) sheet, as received from Martin Marietta Corporation. The nominal composition of 2219 is 6.3 Cu-0.3 Mn-0.2 Zr-0.1 V-0.1 Ti.

TABLE 1 - Compositions, in weight percent, of aluminum-lithium alloys studied.

Alloy	Cu	Li	Mg	Zr	In	Fe	Zn
2090-T6	2.61	2.29	<0.01	0.15	--	0.08	0.03
2090+In-T6	2.64	2.22	<0.01	0.20	0.13	0.11	0.03
2090+In#1,2	2.54	2.30	<0.01	0.18	0.21	0.05	<0.01
8090-T6	1.19	2.46	0.72	0.19	--	0.08	0.02
2090-T81	2.86	2.05	<0.01	0.12	--	0.02	--

Superplastic materials were received from Northrop and processed at both Northrop and LBL. The superplastic forming (SPF) pretreatment, conducted at Northrop, began with hot roll homogenization of the ingot to 1.588 cm (0.625 inches). The plate was then solution heat treated for 30 minutes between 538 and 543°C (1000-1010°F) and cold water quenched. Next the plate was overaged for 16 hours at 413°C (775°F), and, finally, rolled to 0.318 cm (0.125 inch) sheet at 0.318 cm per pass.

After the SPF preparation, additional thermal treatment was applied at LBL. Samples from the second lot of 2090+In (#1 and #2) were held at the forming temperature, 502°C (935°F), for 2 hours and then air cooled. 2090 and 8090 were solution heat treated at 560°C for 15 minutes, while 2090+In was heated at 555°C for 0 to 30 minutes: no heat treatment for the #1 SPF condition, 15 minutes for the #2 SPF tempered condition, and 30 minutes for the T6 condition. The solution temperatures were selected on the basis of differential scanning calorimetry (DSC) and the times were determined through metallographic observations and x-ray fluorescence on the intermetallic particles (11).

Solution treatment was followed, within a few hours, by peak strength aging 2090, 8090, and the first 2090+In lot at 190°C for 16 hours. This aging time was determined by Meyer hardness (11), which is a method using a standard hardness technique, such as Rockwell hardness, for a range of d/D (indentor diameter divided by indentation diameter) which is obtained by varying indentor size and applied load. The method has been used to correlate hardness to strength for Aluminum alloys (16). 2090+In #1 received no aging, while 2090+In #2 was aged near peak strength for 72 hours at 160°C, an aging treatment determined by researchers at NASA using Rockwell hardness test data (12).

The reference materials, 2090-T81 and 2219-T87, are both cold worked, solution-ized, and peak strength aged materials.

Metallography.

Optical metallography was used to determine the relative grain and intermetallic particle morphology. Samples in three perpendicular orientations (long-short, short-transverse, and transverse-long) were mounted and polished to 600 grit with sand papers. They were then polished at 6 μm and 1 μm with diamond paste. The final polish was at 0.6 μm with Mastermet. Specimens were etched using Kellers reagent in the proportions 2.5 % HNO_3, 1.5% HCl, 0.5 % HF, and balance distilled water. For 2090+In #1 and 2, the HF concentration was increased to 1.0 % to better emphasize the grain structure.

Mechanical testing.

Duplicate longitudinal tensile and long-transverse toughness tests were conducted on each material at 300 and 77 K. All tests were done using a stroke rate of 5.1×10^{-4} cm/s (2×10^{-4} in/s) on a hydraulic testing machine. The stroke rate was chosen to emulate that used at Alcoa during the initial Kahn tear test period; however, tests at Alcoa were conducted in load control while those at LBL were stroke rate controlled, thus this was an approximation (17).

Tensile tests were done with flat subsized 2.54 cm (1 in) gage specimens that were taken from the center 0.25 cm (0.1 in) of the 0.318 cm (0.125 in) sheets. Tensile data for 2090-T81 was taken from previous work at LBL on the t /4 tensile properties of 1.27 cm (0.5 in) plate, since the same plate was used for toughness tests (3).

Kahn tear specimens were all taken from the center 0.16 cm (0.063 in) of the sheet materials, and from t /4 of the 2090-T81 plate. Spacers were used to insure proper alignment and no lubrication was used, as an internal Alcoa report claims that lubrication has no significant effect on properties (17). All samples were polished to 600 grit prior to testing and results were obtained by removing data with loads less than or equal to 222 N (50 lbs).

No account was taken for the "angle off transverse" propagation in calculations, as has been done in some studies, and data was not discarded if the crack propagates at angles of greater than 10 degrees, as was done at Alcoa (17). Instead, the toughness comparisons are based on the tear-yield ratio, which is unaffected by the crack path. Individual test information, including angle of propagation, is included in reference (11).

Fracture morphology.

Scanning electron fractographs were made on one side of each type of toughness test to document the fracture appearance and an attempt was made to correlate fracture morphologies to test results and microstructures.

RESULTS AND DISCUSSION

Metallography.

Figure 1 shows the grain structure of the superplastically formable material, 2090+In-T6, which is a mixture of equiaxed, recrystallized grains and elongated, unrecrystallized grains. The other microstructures can be explained by comparison and contrast to the one shown. The extent of recrystallization differs between materials, which probably reflects differences in the uniformity of the deformation. Both conditions of the second lot of 2090+In are primarily composed of small, recrystallized grains, with only a few large, elongated grains. The remaining materials, on the other hand, have alternating layers of recrystallized and unrecrystallized grains, like that shown in the figure of 2090+In-T6. 8090-T6 has the least uniform layering and recrystallization. 2090+In #2, which received the forming anneal and solution treatment, has a slightly larger average recrystallized grain size than the unsolutionized 2090+In #1, indicating more grain growth after recrystallization. Also due to the lack of solution treatment, intermetallic particles are larger and more abundant in 2090+In #1 than in the other materials.

Mechanical testing.

The average longitudinal tensile properties of the aluminum-lithium alloys and the reference material, 2219-T87, are given in Table 2. The yield strength reported is at 0.2 % offset. Table 3 shows the average long-transverse Kahn tear toughness data for the formable Al-Li materials and the reference materials 2090-T81 and 2219-T87.

The strength did increase with the addition of indium to 2090. This is seen by comparing 2090-T6 to 2090+In-T6, which received almost identical processing. In all cases, the strength values increased with decreasing temperature. The ductility of the SPF materials improved or held constant with temperature for all but 2090+In-T6, in which both the elongation and area reduction decreased significantly. Based on tensile data alone, 2090+In #2 is closest to matching the properties of an existing aerospace material, 2219-T87.

Conversely, based on the Kahn tear toughness data, 2090+In #1 is the only material that approximates the toughness of 2219-T87. The trade-off is an example of an important trend that is apparent in a plot of the strength versus the toughness indicator. Figure 2 is a plot of the yield strength against the tear-yield ratio (the 2090-T81 yield strength data used for this plot is from previous work done at LBL (3). Although the strength increases with the indium addition, the strength-toughness combination is not changed favorably.

The alloy 2090+In #1 shows an increase in toughness with decreasing temperature, as shown in Figure 2. This inverse behavior, which has previously been seen in 2090-T81 plate and other Al-Li materials, has been the subject of much research in recent years (1-9). Although the trend is interesting, this particular material condition is not likely to be useful due to its low strength.

The horizontal dashed line in Figure 2, emanating from a tear-yield ratio of 1.0, is a rough dividing line between relatively ductile and relatively brittle materials. Materials with toughness values above the line yielded significantly before evident crack propagation. Of the SPF materials tested, those with higher strength are not significantly above the brittle cutoff; furthermore, after superplastic forming the materials will almost certainly exhibit worse mechanical properties. Thus, for the current set of materials, a strength-toughness combination intermediate to those tested is probably best for the pre-SPF properties, if these properties are acceptable. If not, then possibly new alloy modifications, or entirely new alloys, will be needed. Work on another promising system has been done by the authors and can be found in reference (11).

Comparison of the 2219-T87 results with Alcoa data shows large differences in the unit initiation and propagation energies. The LBL initiation energy is 52 % higher, the propagation energy is 68 % higher, the tear strength is 26 % higher, and the yield strength is 12 % lower, giving a tear yield ratio 44 % higher than at Alcoa. Comparison tests were also conducted on 6061-T6, and the results were such that no trends could be found in the combined discrepancies.

TABLE 2 - Average longitudinal tensile properties of duplicate tests at 300 and 77 K for aluminum-lithium alloys and reference material 2219-T87.

Material	Temp. K	Yield Strength MPa (ksi)	Tensile Strength MPa (ksi)	Total Elongation %	Area Reduction %
2090+In-T6	300	410 (59)	470 (68)	8	12
	77	470 (68)	530 (78)	4	6
2090+In-#1	300	150 (22)	260 (37)	10	19
	77	180 (26)	340 (50)	25	27
2090+In-#2	300	360 (53)	460 (67)	6	12
	77	410 (60)	570 (83)	9	12
2090-T6	300	330 (49)	420 (62)	5	8
	77	380 (55)	530 (77)	15	15
8090-T6	300	330 (49)	430 (63)	9	9
	77	380 (55)	500 (72)	11	12
2219-T87	300	350 (51)	430 (63)	12	33
	77	440 (64)	580 (84)	11	27

TABLE 3 - Average long-transverse Kahn tear toughness properties from duplicate tests at 300 and 77 K for superplastically formable aluminum-lithium alloys and reference materials 2090-T81 and 2219-T87.

Material	Test Temp. K	U.I.E. J/[m*m*100]	U.P.E. (in-lb/in*in)	Tear Strength MPa (ksi)	Tear Yield Ratio
2090+In-T6	300	261 (149)	62 (36)	370 (54)	0.92
	77	89 (51)	26 (15)	220 (33)	0.48
2090+In-#1	300	271 (155)	433 (247)	270 (40)	1.84
	77	459 (262)	770 (440)	330 (49)	1.90
2090+In-#2	300	373 (213)	242 (138)	440 (64)	1.22
	77	176 (101)	73 (42)	380 (56)	0.93
2090-T6	300	251 (144)	155 (89)	370 (54)	1.10
	77	229 (131)	109 (63)	390 (57)	1.04
8090-T6	300	233 (133)	250 (143)	340 (49)	1.01
	77	234 (134)	208 (119)	390 (56)	1.03
2090-T81	300	385 (220)	240 (137)	450 (65)	0.98
	77	451 (258)	382 (218)	510 (75)	0.98
2219-T87	300	590 (337)	632 (361)	510 (74)	1.46
	77	620 (354)	689 (394)	610 (88)	1.39

The large differences in these results suggests that materials tested under different conditions should either not be compared, or the comparison should be taken with consideration of these variations. Several factors could be responsible for the variations including differences in material lot, control mode, machine compliance, and analysis method. The effects of these factors on properties are beyond the scope of this paper and are discussed in reference (11).

Fracture morphology.

Fracture surfaces at two magnifications for the superplastically formable materials are shown in Figures 3-7. In all cases, as seen at the lower magnification, 300 K surfaces were sheared after an initial pop-in (triangular) region, while 77 K surfaces were flat. This sort of transition, which is common in aluminum alloys (14), is probably due in this case to a change to a more uniform deformation pattern with decreasing temperature (i.e. increasing strength), such that at 77 K concentrated 45° slip bands are not present. While Herzberg (14) generally ascribes this morphological change to a transition from plane stress to plane strain, that is unlikely to be the case for the aluminum specimens used here, which were only 0.16 cm (0.063 in) thick with a 2.54 cm (1 in) ligament. The specimens delaminate during fracture at lower temperature. While it has been suggested that delamination should increase the toughness (2, 8), delamination accompanies a decrease in the Kahn tear toughness in this case.

Higher magnification shows that most of the fracture features have sizes on the order of the small, recrystallized grain structure, and are probably intergranular. The alloy 2090+In #1 is an exception. This material fractured via ductile rupture, which concurs with its low strength and high toughness. It also has the most dense intermetallic particle structure and was not solutionized, giving it a large fraction of void initiation sites. Other features, such as large crevices and smooth areas, are probably intergranular delamination of unrecrystallized grains. All surfaces have some regions which appear transgranular, while those of 2090+In-T6, the most brittle material, contain a large fraction of fine rough regions which appear transgranular in nature.

CONCLUSION

Although the addition of indium increases the strength of aluminum-lithium alloys, it does not improve the strength-toughness combination. Whether or not the superplastically formable condition of these alloys can be used in cryogenic tankage will depend on the design property limits, which have not yet been established or publicized. The superplastically formable materials in this study do not compare favorably with 2219-T87 in their strength-toughness combinations; however, designs may be proposed which favor the lower density and higher modulus of aluminum-lithium alloys, and can accept the lower strength and toughness of these materials to take advantage of their superplastic forming characteristics.

ACKNOWLEDGEMENT

The authors are grateful to Judy Glazer, LBL, and Ralph R. Sawtell, Alcoa, for helpful discussions and to Pamela A. Kramer, now at Lockheed Palo Alto, for help with the metallography and fractography. The research on superplastic alloys was supported by a contract with the NASA Langley Research Center. The reference alloy 2219-T87 was donated by Martin Marietta Corporation, while 2090-T81 was donated by Alcoa. Research on the reference alloys was supported by the Director, Office of Energy Research, Office of

Basic Energy Science, Material Sciences Division of the U.S. Department of Energy under Contract No. DE-AC03-76SF00098.

REFERENCES

(1) Glazer, J., Verzasconi, S.L., Dalder, E.N.C., Yu, W., Emigh, R.A., Ritchie, R.O. and Morris, J.W. Jr., Adv. Cryo. Eng., Vol. 32, 1986, pp. 397-404.

(2) Dorward, R.C., Scripta Met., Vol. 20, 1986, pp. 1379 -1383.

(3) Glazer, J., Verzasconi, S. L., Sawtell, R. R. and Morris, J.W. Jr., Metall. Trans., Vol. 18A, 1987, pp. 1695-1701.

(4) D. Webster, Metall.Trans, 18A:2181-2193, 1987.

(5) Morris, J.W., Jr. and Glazer, J., International Cryogenic Materials Conference Proceedings, Shenyang, China, 1988, pp. 713-726.

(6) Jata, K.V. and Starke, E.A. Jr., Scripta Met., 1988, Vol. 22, pp. 1553-1556.

(7) Rao, K.T.V., Hayashigatani, H. and Ritchie, R.O., Scripta Met., Vol. 22, 1988, pp. 93-96.

(8) Rao, K.T.V., Yu, W. and Ritchie, R.O., Metall. Trans., in press.

(9) Glazer, J. and Morris, J.W. Jr., Proc. of Al-Li V, Virginia, 1989.

(10) Silcock, J.M., Heal, T.J., and Hardy, H.K., J. of the Institute of Metals, Vol. 84, 1955-6, pp. 23-31.

(11) Verzasconi, S.L., Masters Thesis, University of California at Berkeley, to be published, May 1989.

(12) Blackburn, L., Cassda, W., Covin, G., Shiflet, G., and Stark, E., Proc. of the 1987 Al-Li Symposium, L.A., ASM, 1987, pp. 187-235.

(13) Kaufman, J.G. and Holt, M., "Fracture Characteristics of Aluminum Alloys," Alcoa Research Laboratories, Technical Paper No. 18, 1965.

(14) Hertzberg, R.W., "Deformation and Fracture Mechanics of Engineering Materials," 2nd Ed., John Wiley & Sons, New York, 1983.

(15) Kaufman, J.G., "Design of Aluminum Alloys for High Toughness and High Fatigue Strength," AGARD Conf. Proc. No. 185, 1975.

(16) Shabel, B.S., U.S. Patent No. 4,530,235, 1985.

(17) Kaufman, J.G. and Reedy, J.F., "Description and Procedure for Making Kahn-Type Tear Tests," Internal Alcoa Research Laboratory Report No. 9-M-681, 1966.

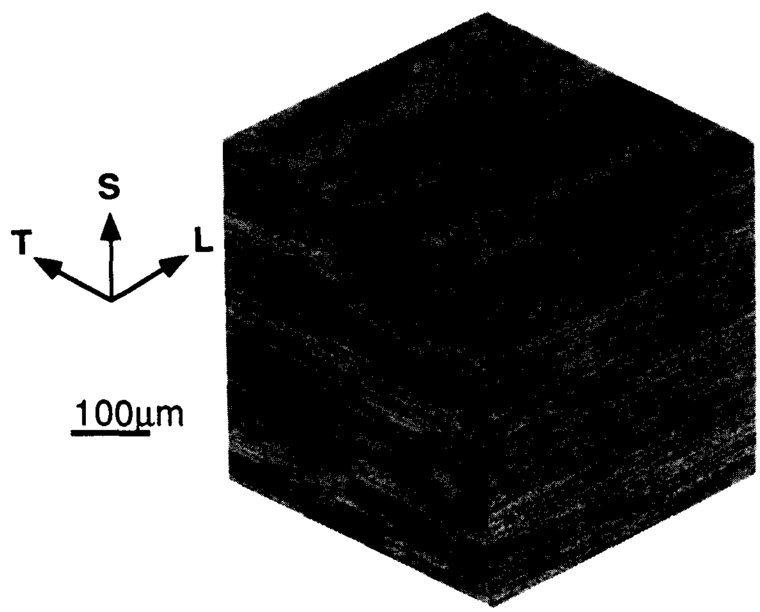

XBB 892-865, middle figure

Figure 1: Metallography shows the grain structure of superplastically formable material 2090+In-T6.

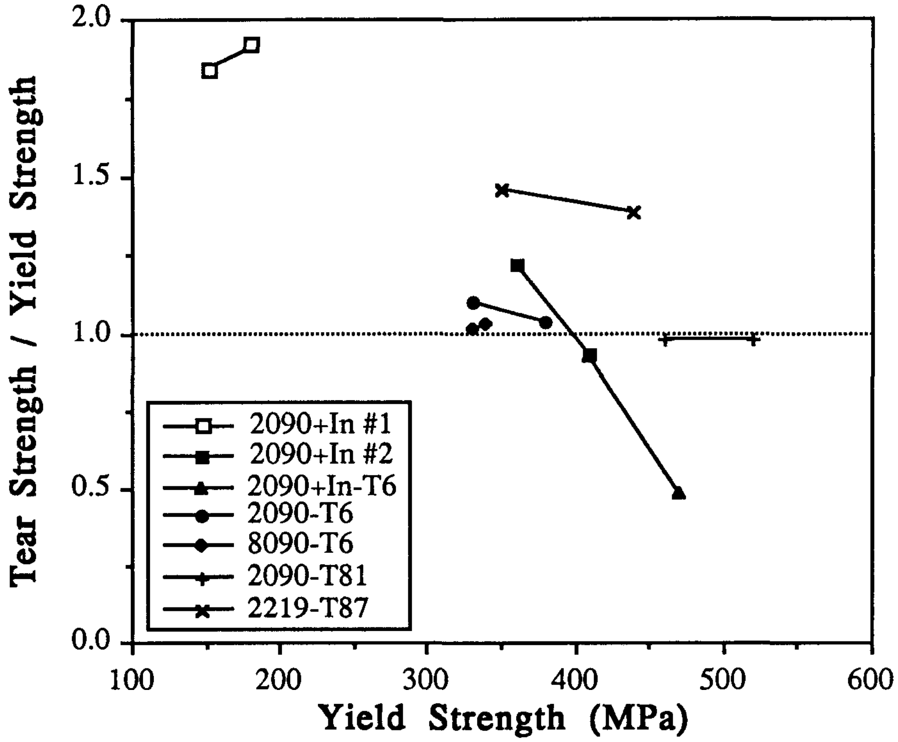

Figure 2: Strength-toughness values of superplastic materials are compared to 2090-T81 and 2219-T87. Lower strength data corrisponds to 300 K tests, higher, to 77 K.

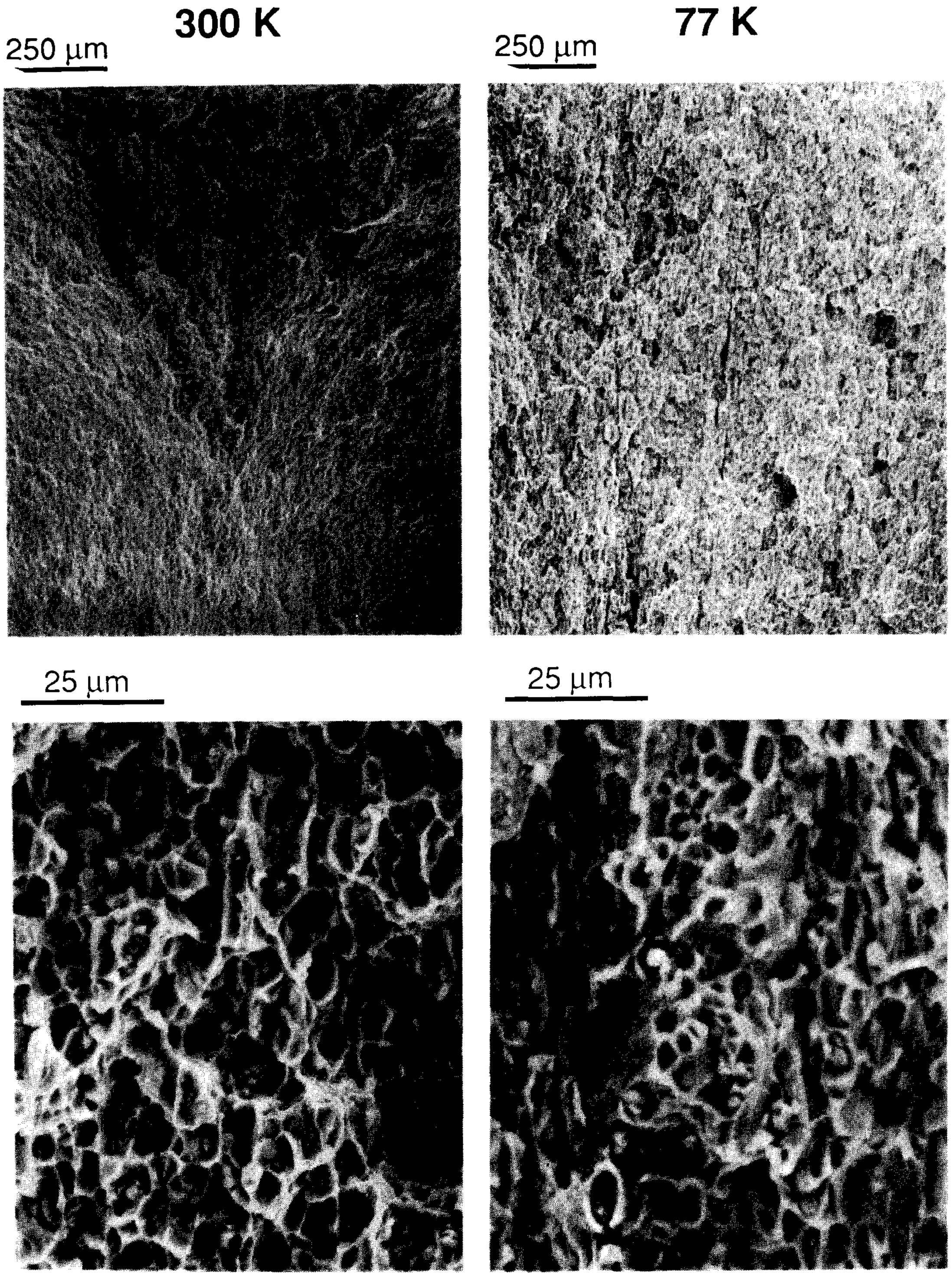

XBB 892-875

Figure 3: Scanning electron micrographs of 2090+In #1 Kahn tear specimens tested at 300 and 77 K. Top photographs are lower magnification than bottom ones; left column photographs are from 300 K tests while right column ones are from 77 K tests.

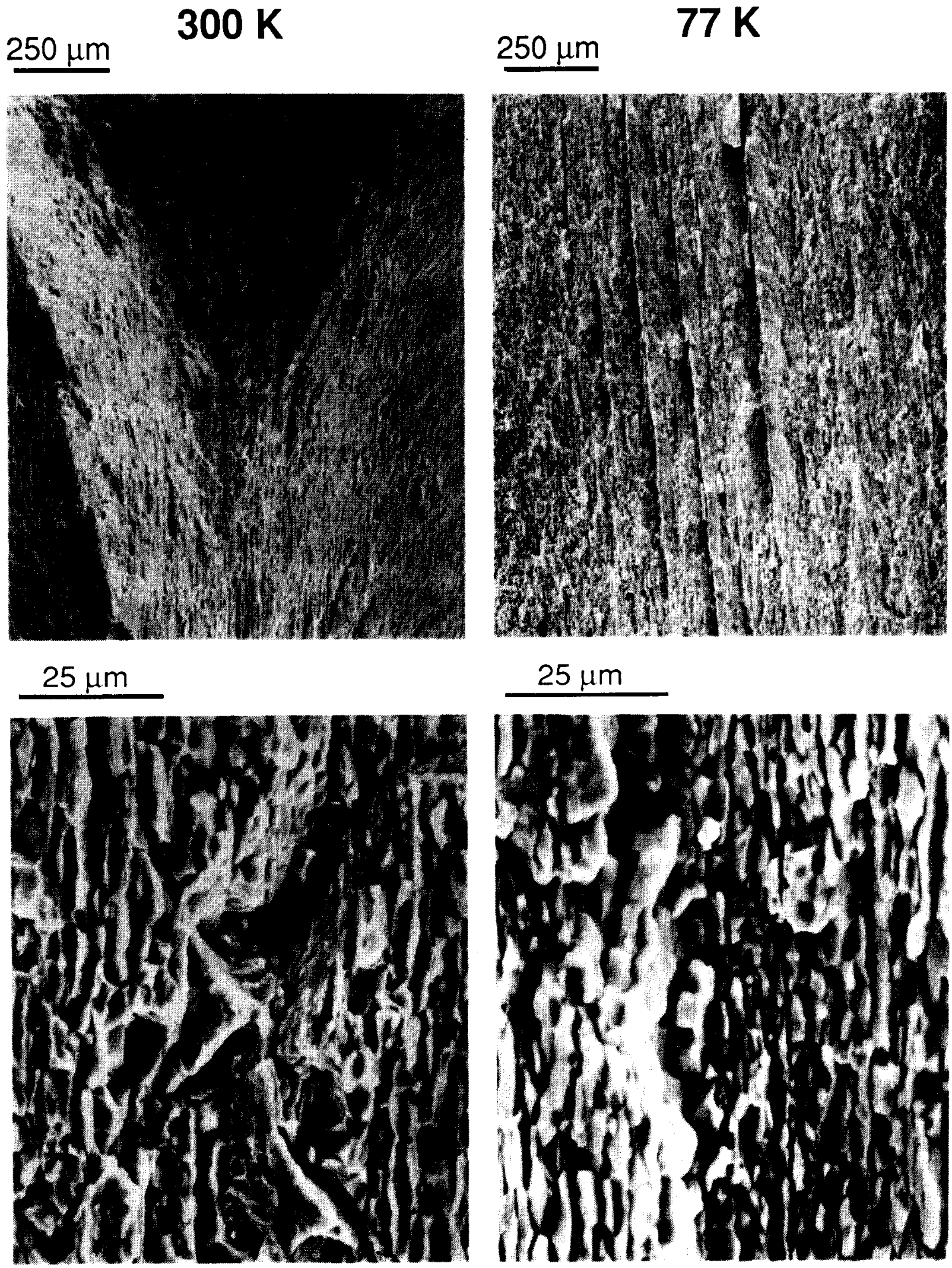

XBB 892-874

Figure 4: Scanning electron micrographs of 2090+In #2 Kahn tear specimens tested at 300 and 77 K. Top photographs are lower magnification than bottom ones; left column photographs are from 300 K tests while right column ones are from 77 K tests.

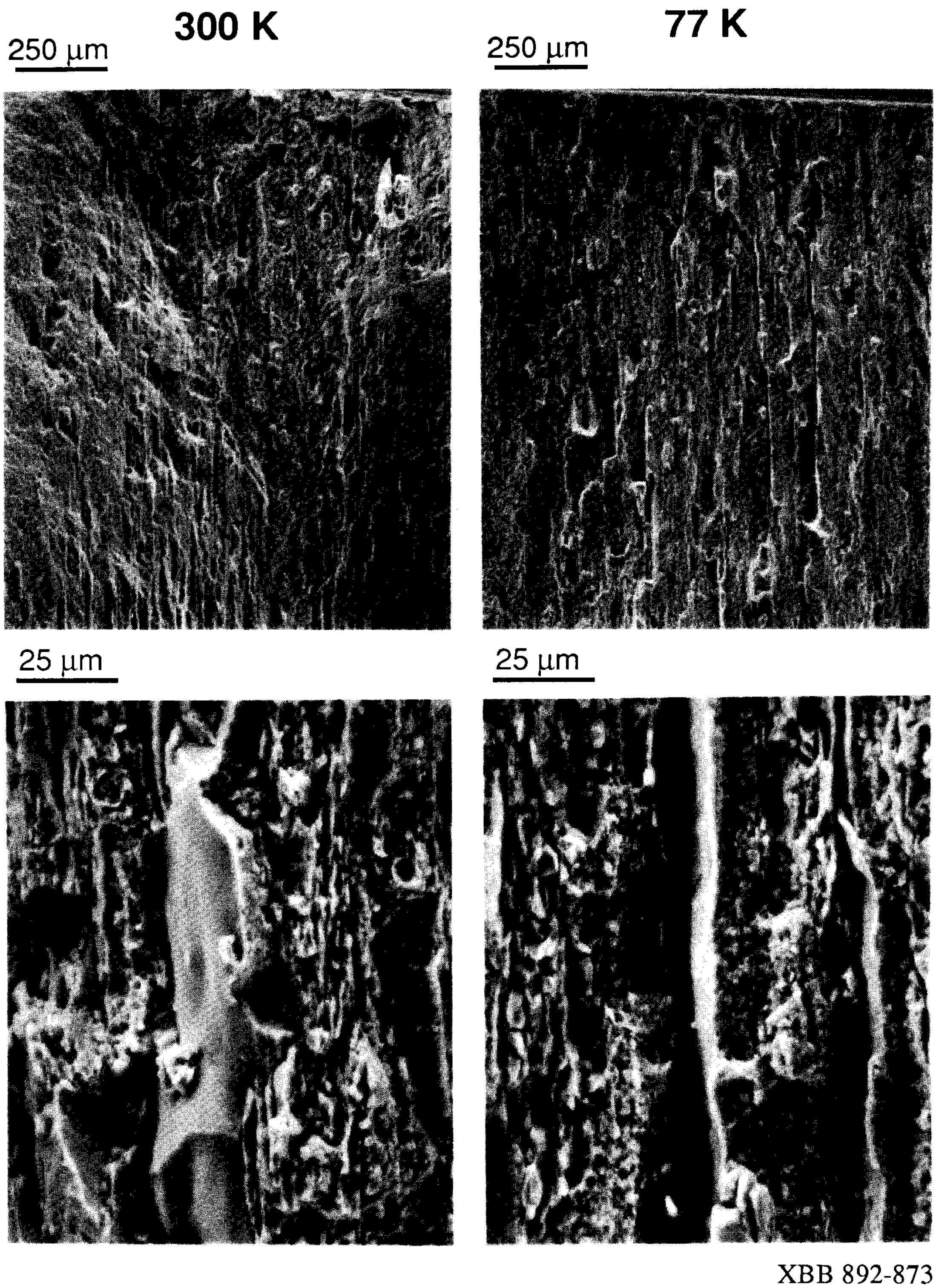

Figure 5: Scanning electron micrographs of 2090+In-T6 Kahn tear specimens tested at 300 and 77 K. Top photographs are lower magnification than bottom ones; left column photographs are from 300 K tests while right column ones are from 77 K tests.

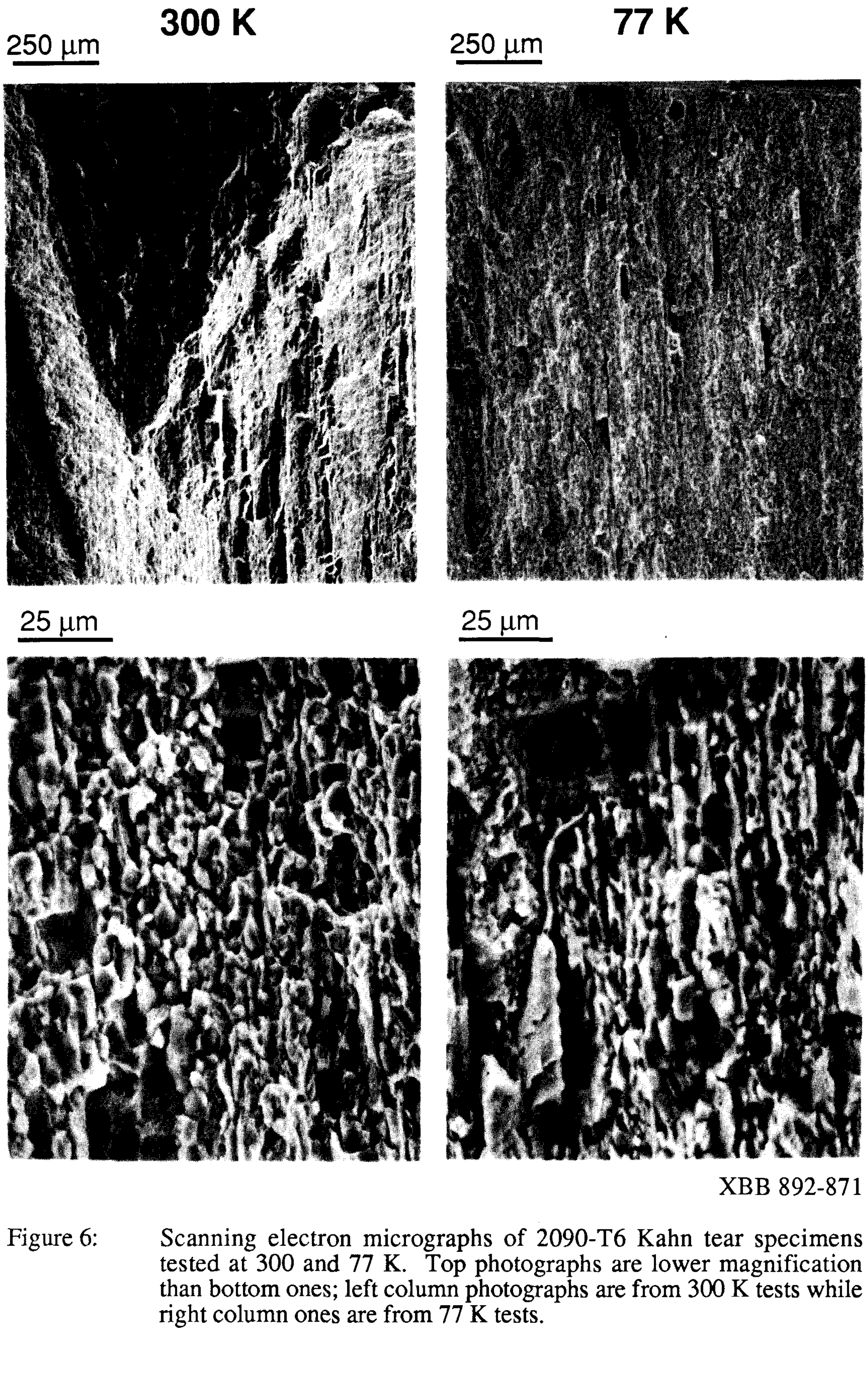

XBB 892-871

Figure 6: Scanning electron micrographs of 2090-T6 Kahn tear specimens tested at 300 and 77 K. Top photographs are lower magnification than bottom ones; left column photographs are from 300 K tests while right column ones are from 77 K tests.

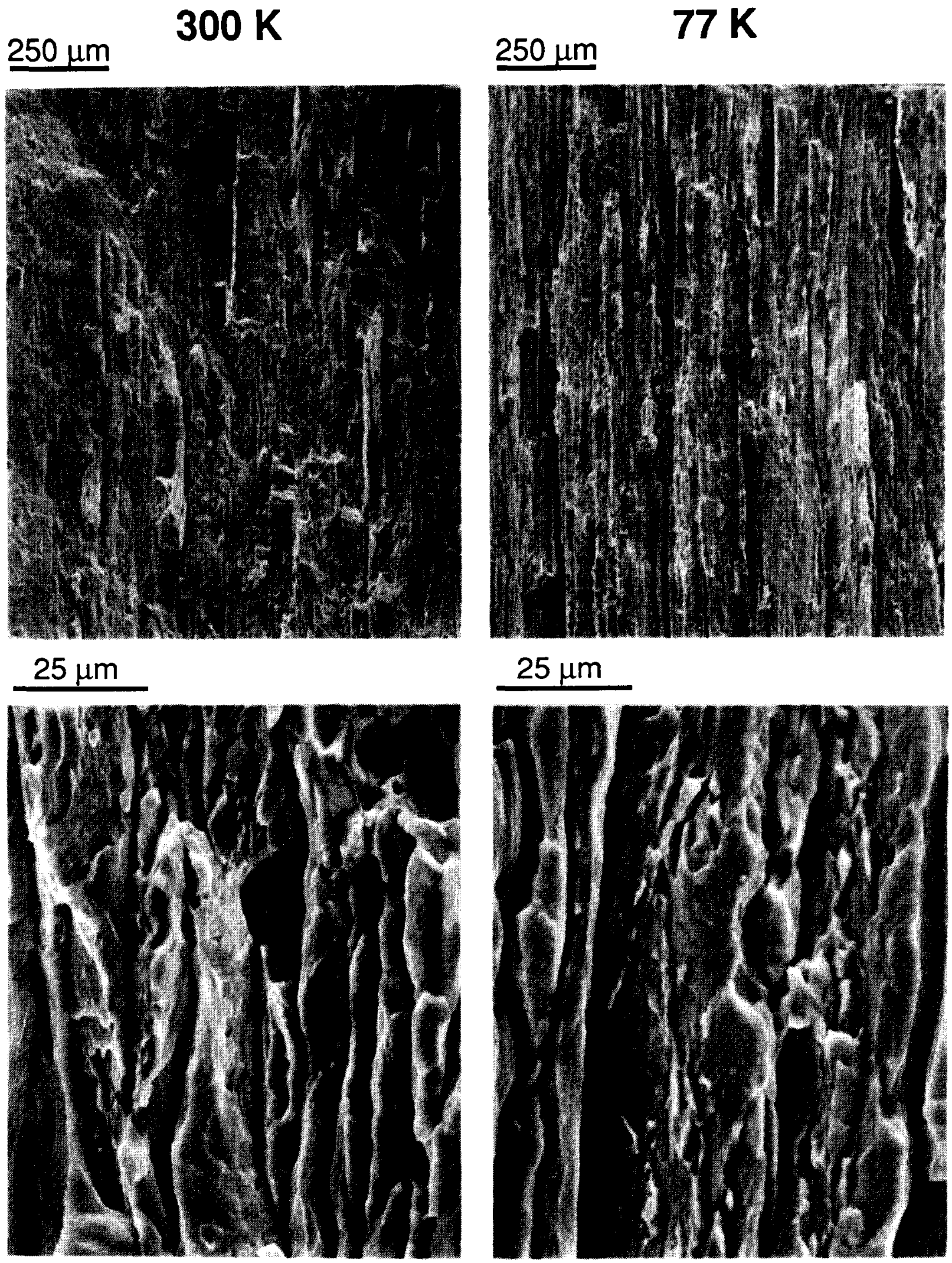

XBB 892-872

Figure 7: Scanning electron micrographs of 8090-T6 Kahn tear specimens tested at 300 and 77 K. Top photographs are lower magnification than bottom ones; left column photographs are from 300 K tests while right column ones are from 77 K tests.